Геология и геофизика, 2022, т. 63, № 5, с. 764—779

УДК 622.732(514)

УГОЛЬНЫЕ ПОЖАРЫ В РАЙОНЕ ЛЮХУАНГОУ (*Синьцзян, Северо-Западный Китай*) В ПОЗДНЕМ КАЙНОЗОЕ: ВОЗРАСТ, КОНТРОЛИРУЮЩИЕ ФАКТОРЫ И РАЗВИТИЕ

Б. Чэнь[a,b], М. Франчески[c], Я. Ван[d], С. Дуань[e], С. Цзинь[b], Ч. Ши[a,b]

[a]*State Key Laboratory of Oil and Gas Reservoir Geology and Exploitation, Chengdu University of Technology, Chengdu, 610059, China*

[b]*Institute of Sedimentary Geology, Chengdu University of Technology, Chengdu, 610059, China*

[c]*Department of Mathematics and Geosciences, University of Trieste, via E. Weiss 2, Trieste, 34128, Italy*

[d]*College of Materials, Chemistry and Chemical Engineering, Chengdu University of Technology, Chengdu, 610059, China*

[e]*School of Land and Resources, China West Normal University, Nanchong, 637009, China*

Угольные пожары — явление, наблюдаемое по всему миру в регионах, где обнажены породы с угленосными слоями, которое может представлять существенную угрозу для окружающей среды. Угольные пожары могут возникать за счет самовозгорания, когда угли обнажаются в сухих богатых кислородом приповерхностных условиях. В зависимости от температуры нагрева, горение вызывает прокаливание или даже плавление окружающих пород и приводит к образованию различных типов горелых пород. В северо-западном Китае проявления угольных пожаров сосредоточены на окраинах осадочных бассейнов или на краевых частях орогенных поясов, где богатые углем толщи были обнажены в результате индо-евразийской коллизии. На северной окраине хребта Тянь-Шань имеются распространенные признаки угольных пожаров в юрских угленосных осадочных толщах, проявленных вдоль Центрально-Азиатского складчатого пояса. В некоторых случаях происходят активные пожары, которые могут быть связаны с современной деятельностью горнодобывающих предприятий, но существуют также коренные выходы метаморфических горелых пород, не связанных с современными пожарами, что указывает на древние процессы горения. В настоящей статье рассматриваются метаморфические горелые породы, обнаженные в долине реки Тотунхе (район Люхуангоу, Синьцзян, северо-западный Китай). В районе исследования метаморфические горелые породы были закартированы и классифицированы в соответствии с их морфологическими и минералогическими характеристиками. Коренные выходы проявлены на различной высоте в бортах реки, которые характеризуются наличием многочисленных уровней флювиальных террас. Последние указывают на фазы эрозии и отложения в реке Тотунхе и свидетельствуют о тектоническом поднятии. Исследование стратиграфических и секущих взаимоотношений метаморфических горелых пород с отложениями террас и датирование по следам распада в апатите позволяют установить, что имели место как минимум четыре фазы горения угля, от позднего миоцена до четвертичного периода. Первая, самая древняя фаза горения имеет возраст 10.0 ± 1.3 млн лет и завершилась к 2–3 млн лет назад. Вторая фаза была активна приблизительно до 550 тыс. лет назад. Третья фаза закончилась примерно к 140 тыс. лет назад. Четвертая фаза началась позднее 5.7 тыс. лет назад. Кроме того, взаимоотношения между метаморфическими горелыми породами и флювиальными террасами указывают на то, что возгорание и затухание угольных пожаров в регионе, начиная с миоцена, могли быть связаны со сменой поднятия коры в Центрально-Азиатском складчатом поясе фазами флювиальной эрозии и осадконакопления в межледниковые периоды.

Поздний кайнозой, угольный пожар, метаморфические горелые породы, апатит, датирование по следам распада, геоморфологическая эволюция

LATE CENOZOIC COAL FIRES IN THE LIUHUANGGOU AREA (*Xinjiang, Northwestern China*): AGES, CONTROLLING FACTORS AND EVOLUTION

B. Chen, M. Franceschi, Y. Wang, X. Duan, X. Jin, Z. Shi

Coal fires are a phenomenon that can be observed worldwide in areas where rocks containing coal seams are exposed and can pose major environmental threats. A coal fire can begin through spontaneous combustion when coals are exposed to dry and oxygen-rich near-surface conditions. Burning, depending on the temperature of heating, causes baking or even melting of the surrounding rocks and the formation of different types of combustion metamorphic rocks. In Northwestern China, coal fire occurrences are concentrated at the edges of the sedimentary basins or at the margins of orogenic belts, where coalrich units were exposed owing to the Indo-Eurasian collision. On the northern margin of the Tianshan range, evidence of coal fires is widespread in the Jurassic sedimentary units containing coal seams which outcrop along the Central Asian Orogenic Belt. In

✉e-mail: sqzcdut@163.com

DOI: 10.15372/GiG2020166

some cases, coal fires are active and can be linked to ongoing mining activity, but outcrops of combustion metamorphic rocks not associated with fires are also found and are indicative of past burning events. We examine combustion metamorphic rocks outcropping in the Toutunhe River valley (Liuhuangou area, Xinjiang, Northwestern China). Combustion metamorphic rocks in the study area were mapped and classified according to their morphological and mineralogical characteristics. Outcrops are exposed at various heights on the valley flanks, which are characterized by the presence of multiple levels of fluvial terraces. These terraces are indicative of the phases of erosion and deposition of the Toutunhe River and testify to tectonic uplift. The investigation of the stratigraphic and crosscutting relationship of combustion metamorphic rocks with terrace deposits and apatite fissiontrack dating made it possible to determine that at least four phases of coal fire activity occurred from late Miocene to Quaternary. The first and oldest burning phase dates back to 10 ± 1.3 Ma and terminated prior to 2–3 Ma; the second was active before ~550 ka; the third had terminated by ~140 ka; the fourth began later than ~5.7 ka. The relationships between combustion metamorphic rocks and fluvial terraces further suggest that coal fire ignition/extinction in the area since the Miocene have been linked to the interplay between the uplift of the Central Asian Orogenic Belt and the phases of fluvial erosion and deposition in interglacial periods.

Coal fire, combustion metamorphic rocks, apatite fission-track dating, geomorphologic evolution, late Cenozoic

INTRODUCTION

Coal fires are a phenomenon in which coal contained in sedimentary rocks ignites and then burns in the near-surface layer for an indefinite time. Ignition may be natural (e.g., because of spontaneous combustion, forest fires, and lightning strikes) or anthropogenic (e.g., because of mining activities) (Wang et al., 2003; Silva and Boit, 2011), and surface exposure of coal seams and therefore the availability of oxygen is considered a necessary condition for the development of a coal fire (Zhang et al., 2004). Coal fires are observed worldwide: in China, India, United States, Russia, and South Africa (Stracher, 2007; Kuenzer and Stracher, 2012; Song and Kuenzer, 2014; Stracher et al., 2015; Ribeiro et al., 2016). Coal fires can in some cases represent a threat if there is significant emission of gases and particulate matter potentially dangerous for the environment and humans (Stracher and Taylor, 2004; Kuenzer and Stracher, 2012; Song and Kuenzer, 2014, 2017).

Coal fires are common in northwestern China because of the abundance of coal-bearing geologic units. The ignition is facilitated by the intense quarrying activity of coal seams and by the arid climate conditions (Stracher and Taylor, 2004; Querol et al., 2008; Song and Kuenzer, 2014). Coal fires in northwestern China are particularly concentrated at the edges of the sedimentary basins (e.g., the Ordos, Tuha, Yili, Tarim, and Junggar basins) or at the margins of orogenic belts (e.g., the Tianshan Orogen) (Kuenzer et al., 2007; Sokol and Volkova, 2007). In these regions, the coal seams were exposed by uplift and erosion, and this created the conditions for combustion.

Most studies focused on the factors of spontaneous combustion of coals and detection and extinguishing of modern coal fires (Hoffmann et al., 2003; Voigt et al., 2004; Song and Kuenzer, 2017). Less attention was paid to the investigation of paleo-coal fires, though their existence is indicated by combustion metamorphic (pyrometamorphic) rocks, i.e., rocks that were metamorphosed by heat generated by coal fires, in the geologic record (Heffern and Coates, 2004). Combustion metamorphic (CM) rocks can be produced by heating and/or melting of rocks that host coal fires and therefore are subjected to low- to high-temperature, low-pressure metamorphism. This process results in mineralogical modification caused by dehydration and/or oxidation that can be macroscopically manifested in color and texture changes (Stracher et al., 2015). CM rocks are often relatively resistant to erosion and therefore can build morphological reliefs, such as escarpments and terraces (Heffern et al., 2007; Riihimaki et al., 2009).

The ages of formation of CM rocks and therefore the time they were metamorphosed by active coal fires can be dated with zircon fission tracks, zircon (U–Th)/He dating, or $^{40}Ar/^{39}Ar$ dating (Gur et al., 1995; Heffern et al., 2007; Novikov et al., 2008; Sokol et al., 2014; Novikova et al., 2016). $^{40}Ar/^{39}Ar$ dating of CM rocks in Central Asia, especially in the areas of the Goose Lake and Kuznetsk Coal Basins, has revealed that large-scale coal fires occurred in two stages, in the Early and Late Pleistocene (Novikov and Sokol, 2007; Novikov et al., 2008; Novikov, 2013; Sokol et al., 2014; Novikova et al., 2016).

Along the northern margin of the Tianshan mountain range, northwestern China, CM rocks are widespread (Novikov and Sokol, 2007; Novikov et al., 2013) (Fig. 1*b*) and tend to form morphological relief units that were exposed by river erosion. This provides an unusual opportunity to study the ages and evolution of paleo-coal fires in the area. In this paper we present the ages of CM rocks in the Liuhuanggou area, Xinjiang Province, through apatite fission tracks and investigate the time and possible cause–effect relationship between the formation of CM rocks and the erosion/deposition history of the Toutunhe River valley.

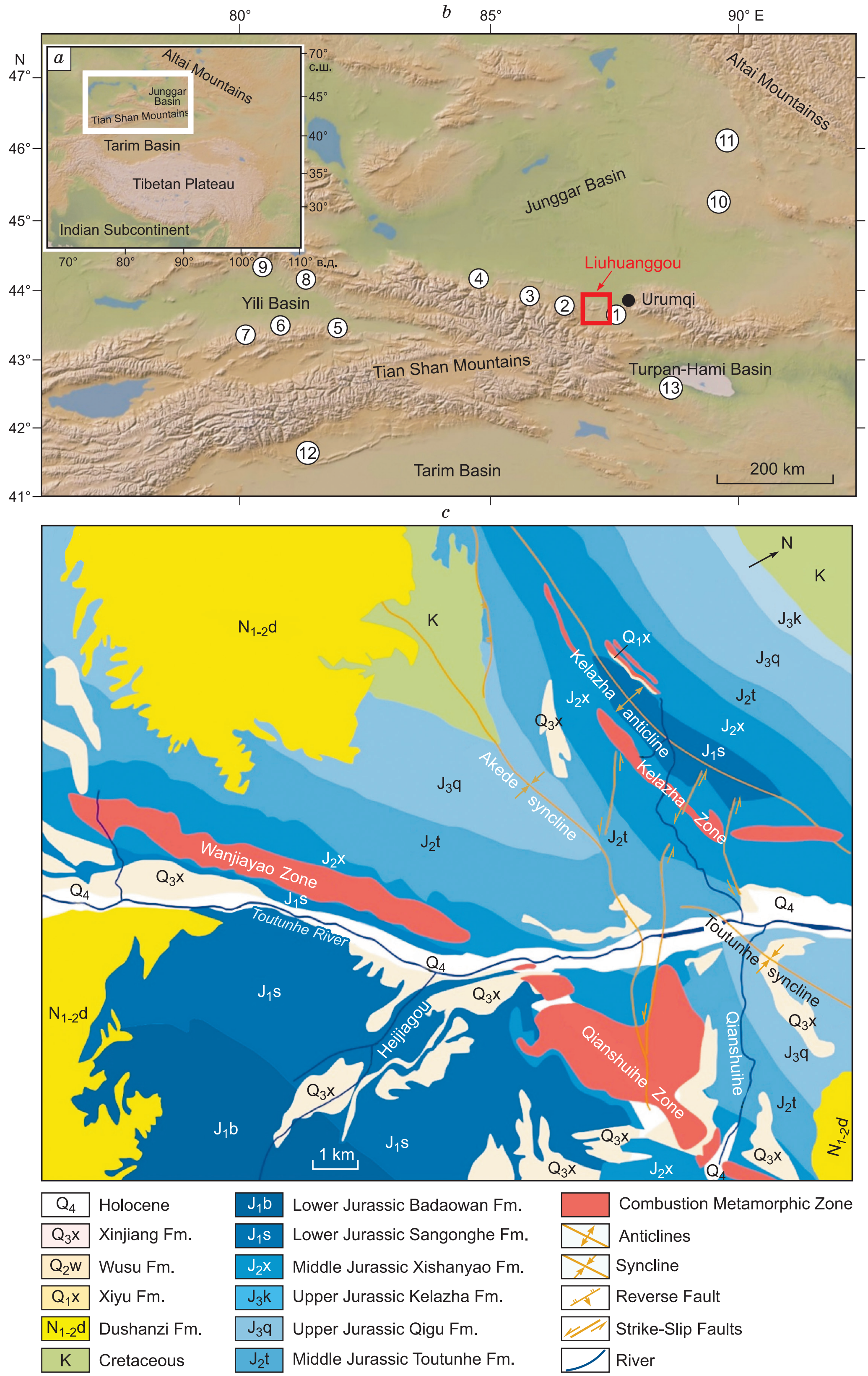

Fig. 1. Topographic map of Central Asia (*a*); *b*, location map of CM rocks and study area in Northwestern China.

1–4, Northern Tianshan piedmont; 5–9, Yili basin; 10–11, eastern margin of the Junggar basin; 12, north margin of the Tarim basin; 13, Turpan–Hami basin (Novikov and Sokol, 2007; Novikov, 2013); *c*, geological map of the Liuhuanggou area, showing the distribution of combustion metamorphic rocks (Guan et al., 1998; Li et al., 2011b).

GEOLOGIC SETTING

In China, the Tianshan Orogenic Belt extends for more than 1700 km with a north–south width of 250–300 km (Fu et al., 2003; Wang et al., 2003). In response to the India–Eurasia collision during the Cenozoic (Dobretsov et al., 1996; Grave et al., 2007; Delvaux et al., 2013), the Tianshan belt has been one of the most active intracontinental mountain-building belts in Central Asia (Fig. 1*a*, *b*) (Molnar and Tapponnier, 1975; Avouac et al., 1993; Fu et al., 2003; Sun and Zhang, 2009; Gong et al., 2015; Glorie and De Grave, 2016). Therefore, the Mesozoic to Cenozoic sedimentary sequences in the northern piedmont of the Tianshan belt have been intensely deformed (Avouac et al., 1993), forming three parallel rows of fold and thrust fault belts (Lu et al., 2010b). These three tectonic belts were termed as Belts I, II, and III from the mountain front sequentially toward the Junggar Basin (Fig. 5), a larger foreland basin in the Xinjiang Province (Fu et al., 2003; Scharer et al., 2004; Sun and Zhang, 2009; Chen et al., 2010; Xu et al., 2015). The anticlines in the belts have approximately west–east-striking axes, indicating a north–south compression (Gong et al., 2014). The study area is characterized by several rows of near-NW–SE-trending anticlines and synclines (Huang et al., 2016), including the Kelazha Anticline, the Akede Syncline, and the Toutunhe Syncline (Fig. 1*c*). Compressive faults are commonly seen in the Liuhuanggou area, and torsional reverse faults mainly develop in the core of anticlines (Guo et al., 2007; Li et al., 2011b). In addition, several strike-slip faults are found in the study area (Li et al., 2011b). In the present study, the major section, the Liuhuangou section, is located at the Kelazha Anticline and belongs to Belt I (43°42′40″ N, 87°12′46″ E) (Fig. 1*b*, *c*). The study area is within the transition zone between Tianshan Mountain and Junggar Basin (Liu et al., 2017).

Figure 1*c* shows a geological map of the study area. The coal-bearing sequences include the Middle Jurassic Xishanyao Formation and the Lower Jurassic Sangonghe and Badaowan Formations (Wu et al., 2012; Zhou et al., 2015). The main coal-bearing intervals are found in the lower Xishanyao Formation (Jiang et al., 2010; Sun et al., 2012; Li et al., 2016). The Jurassic and Cretaceous successions mainly crop out in the Liuhuanggou area, unconformably covered by the Neogene and Quaternary deposits which are mainly found along the valleys of the Toutunhe River and its tributaries (Fig. 1*c*) (Kong et al., 2006; Fang et al., 2007; Zhang, 2015). The Neogene Taxihe (N_1t) and Dushanzi Formations ($N_{1\text{-}2}d$) comprise fluvial facies (Li et al., 2011b). The Quaternary is represented by the Pleistocene Xiyu (Q_1x), Wusu (Q_2w), and Xinjiang (Q_3x) Formations. These units are mainly made up of poorly cemented conglomerates of the alluvial facies, and the Xinjiang Formation typically forms fluvial terraces. Holocene alluvial deposits made up of gravels, sands, and loess represent the more recent infill of the river valley (Q_4) (Fu et al., 2003, 2017; Li et al., 2011b).

METHODS

Field investigation and geomorphologic analysis

Field investigations were carried out with Google Earth imagery and a 1:80,000 scale geological map (Guan et al., 1998). Based on the reconnaissance and geomorphological mapping, we mapped the distribution of CM rocks in the study area and identified fluvial terraces. Moreover, we identified the types of CM rocks based on petrology, which were reflected by mineral composition and the grade of thermal alteration.

Apatite fission-track dating

The CM rocks have commonly been heated to over 500 °C (Sokol and Volkova, 2007), and as a part of low-temperature thermochronology, apatite fission-track dating is extremely sensitive to changes in temperature. Once the temperature of a sample is over 120 °C, the AFT age will be reset and record the thermal events, so that the application of this technique to CM rocks can represent the age of the coal fires that produced them (Heffern and Coates, 2004).

Two samples (S1 and S2) were collected from the CM rocks outcropping in the study area. The sampling locality is shown in Figs. 1*c* and 3*a*, *b*. The collected samples were crushed, and the apatite grains were separated using heavy liquids and magnetic separation techniques and then selected out under the binocular microscope. Mounts of apatite in epoxy were polished and then etched with 5 M HNO_3 at 20 °C for 20 s. Samples were then irradiated in the well-thermalized reactor with a CN-5 dosimeter at the Radiation Center of Oregon State University (United States). After irradiation-induced fission tracks were revealed in the low-U muscovite detector by etching in 40% HF at 20 °C for 40 min. Apatite fission-track analyses were carried out under a magnification of 1000 with dry objectives. The age calibration uses Durango standard with a zeta value equal to 346.73±1.47.

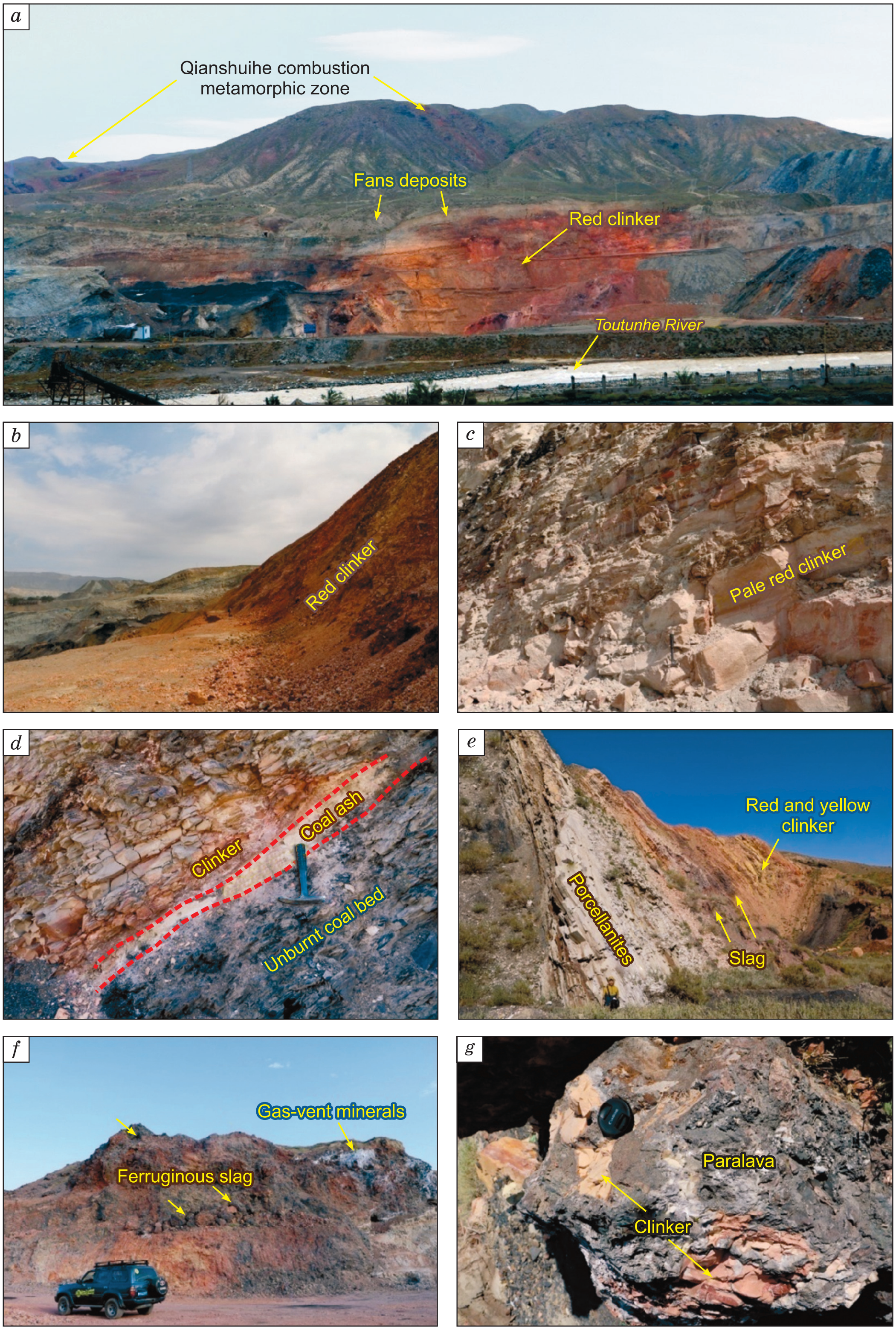

Fig. 2. Photographs of combustion metamorphic rocks.

a–c, Clinker converted to red and pale red owing to spontaneous combustion of the coal in the Qianshuihe combustion metamorphic area; *d*, unburnt coal bed near the bottom of the photo, coal ash in the middle, and clinker in the upper part; *e*, clinker, slag, and porcellanites in the Kelazha combustion metamorphic area; *f*, ferruginous slag formed during the spontaneous combustion of coal beds; *g*, combustion metamorphic breccias and a red clinker fragment cemented by massive black paralava.

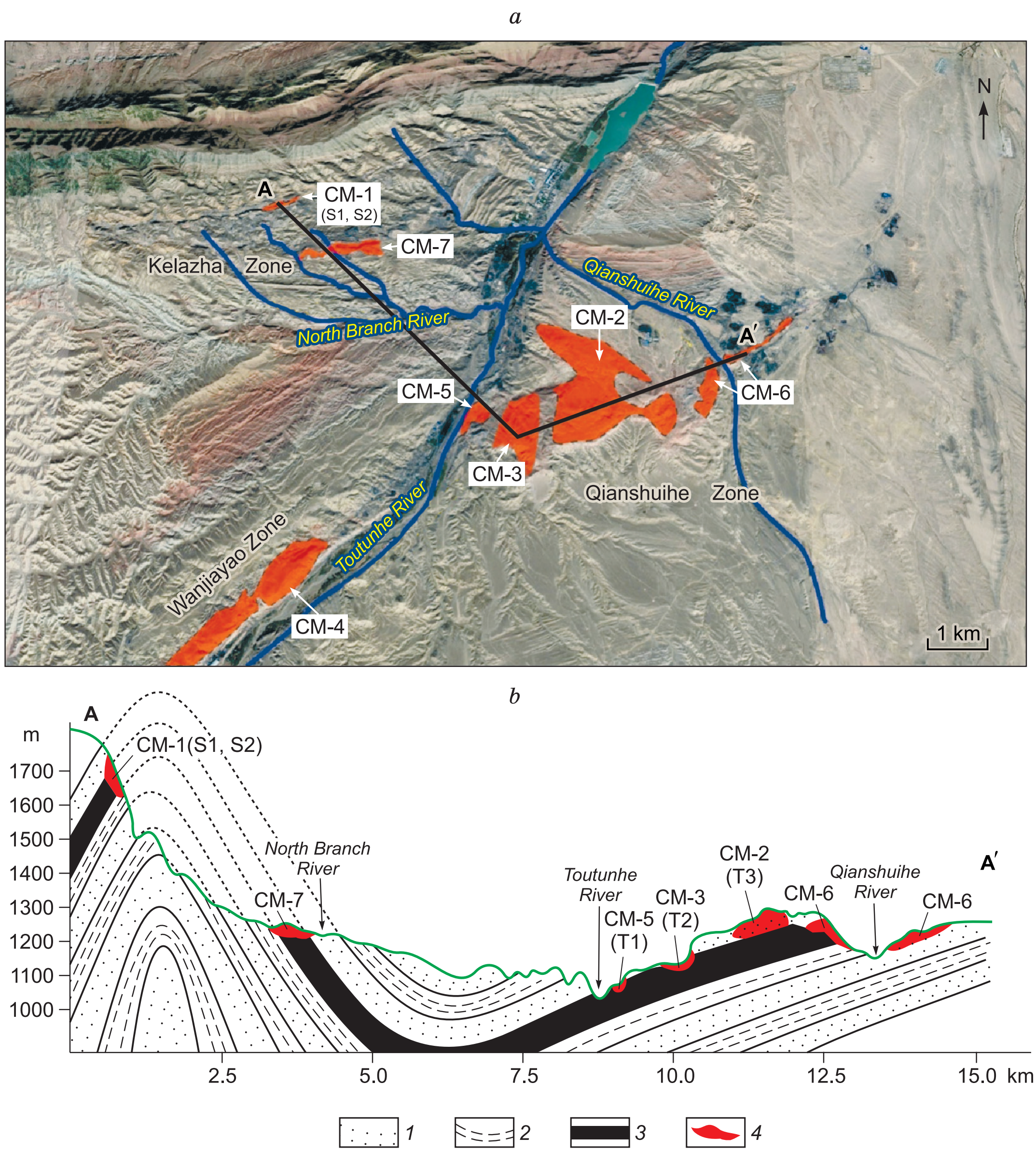

Fig. 3. The distribution of CM rock outcrops (CM-1 and -7) on the Global Mapper of the Liuhuanggou area (*a*); *b*, cross section (A–A′) across the Toutunhe River (terrain data from Global Mapper), showing CM rock outcrops, coal beds, and fluvial terraces (T1–T3).

RESULTS

Characteristics and distribution of combustion metamorphic rocks in the Liuhuanggou area

The types of CM rocks identified in the study area are clinkers (Fig. 2*a*–*c*), porcellanites, (Fig. 2*e*), and paralavas (Fig. 2*f*, *g*). All the CM rocks are characterized by multicolored glassy porcelain or bricklike appearance.

The clinkers were baked at a relatively low temperature. They were mainly found in the Kelazha area, and the most distinctive feature of the clinker is its red color (Figs. 2*a*–*c*). The porcellanites are commonly found in contact with the clinkers. They are dense, hard, partly or completely sintered clays of porcelain-like appearance (Fig. 2*e*). The paralavas, completely fused rocks, are mainly distributed on both sides of the Qianshuihe River. The paralavas also lie directly above the coal ash in the form of thin veinlets or occur as cement fragments of vitreous clinkers called combustion metamorphic breccias (Figs. 2*f*, *g*).

CM rocks are found along the Toutunhe River or exposed on topographic scarps. In addition to the CM rocks, some other products linked to the spontaneous combustion of coal that can be found in the study area are gas-vent minerals (e.g., sulphur and sal ammoniac (Fig. 2*f*)), coal tar, and coal ash layers (Fig. 2*d*)

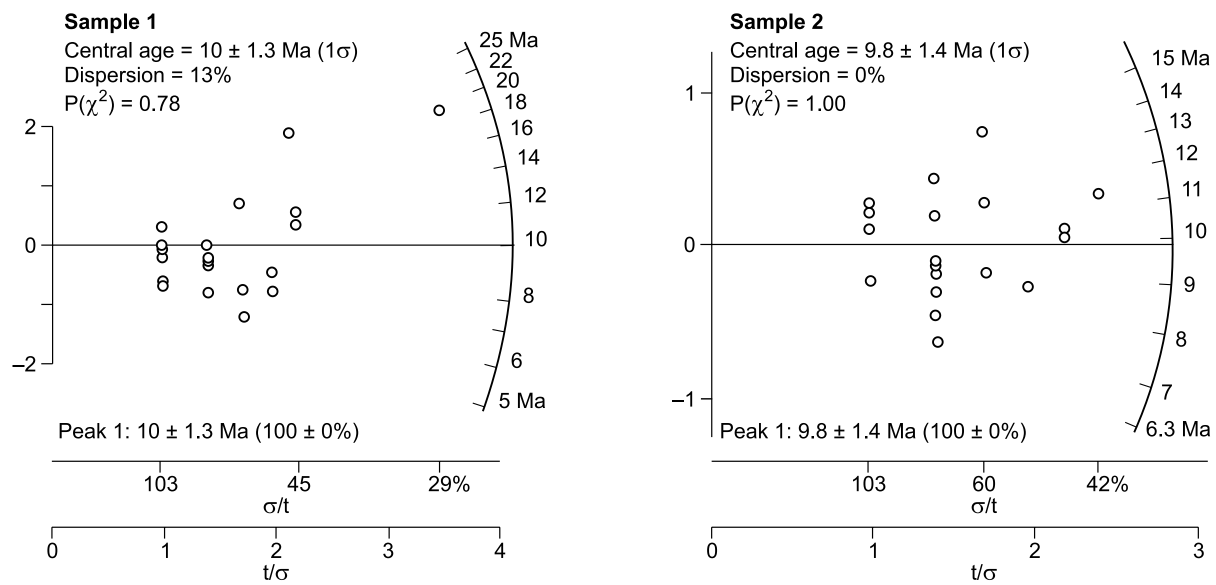

Fig. 4. The radial plot of AFT ages.

Three main CM rock areas have been identified: the Wanjiayao, Qianshuihe, and Kelazha areas (Fig. 1*c*).

The Wanjiayao area is located in the upper reaches of the west bank of the Toutunhe River and is elongated along the fluvial terraces (CM-4) (Fig. 3). The length is about 7.5 km, and the width is about 0.42 km. Owing to the combustion of coal seams, a large number of subsidence fissures are formed on the surface, and some fissures directly communicate with the lower coal seam. These cracks promote combustion by permitting oxygen to circulate to burning coal in the subsurface.

The Qianshuihe area is located on the east bank of the Toutunhe River (including CM-2, -3, -5, and -6). The CM rocks are widely distributed on a surface of approximately 7.02 km^2 (Fig. 1*c*). The distribution of the CM rocks is related to fluvial terraces (Fig. 3).

The Kelazha area is located in the two limbs of the Kelazha Anticline (including CM-1 and -7 (Fig. 1*c*)). CM-1 is located on the north wing of the Kelazha Anticline, and the CM rocks are mainly distributed near the steeply dipping. CM-7 is located on the other wing of the Kelazha Anticline. White smoke is visible, and some minerals nucleated along cracks and vents of CM rocks.

Apatite fission tracks

Our apatite fission-track ages (S1 and S2) show a small range from 5 to 24.5 Ma with central ages of 10 ± ± 1.3 and 9.8 ± 1.4 Ma (Fig. 4). The χ^2 probability P (χ^2) = 0.78 and 1, and this indicates that the samples contain a rather homogeneous age population and the apatite grains underwent annealing because of the same event.

DISCUSSION

Control factors of spontaneous combustion of coal seams

As exposure of coal seams is needed to create conditions for the ignition of coal fires (Riihimaki et al., 2009; Reiners et al., 2011; Sokol et al., 2014; Novikova et al., 2016), the understanding of the age of tectonic uplift and erosion history in the Liuhuanggou area can help to constrain the time of spontaneous combustion phases.

Tectonic uplift

The Tianshan range uplift is related to the India–Eurasia collision, which led to intense structural deformation and erosion (Molnar et al., 1993; Tapponnier et al., 2001). The onset of the uplift of the Tianshan range has been dated between 10 and 7 Ma (Charreau et al., 2005; Fang et al., 2007; Ji et al., 2008; Li et al., 2011b). Magnetostratigraphic studies and stratigraphic relationships indicate that the formation of folds and thrusts occurred roughly between the Miocene and Early Pleistocene (Sun et al., 2004; Daëron et al., 2007; Sun and Zhang, 2009; Fu et al., 2017). Furthermore, Li et al. (2011a,b) suggested that the uplift ages become younger from south to north, and therefore a relative age can be attributed to structural Belts I to III, Belt I being the oldest and Belt III the youngest. Based on the field research and seismic interpretations, Guo et al. (2006) and Chen et al. (2007) suggested that the uplift of Belt II and Belt III occurred after the deposition of the Xiyu Formation. The age of the Xiyu Formation was determined at about 2.58 Ma through magnetostratigraphy (Sun et al., 2004; Charreau et al., 2009). Li et al. (2011b) inferred that the accelerated folding of the anticlinal belts took place at approximately 2 Ma for Belt II (Tugulu Anticline) and at about 1 Ma for Belt III (Anjihai Anticline), according to the identified growth strata dated with the existing magnetostratigraphy, together with balanced cross sections from the interpreted seismic data. Fang et al. (2007) and Li et al. (2011a) suggested that the intense uplift and structural deformation of the Kelazha Anticline (the location of the study area, belonging to Belt I) began in the middle–late Miocene based on the studies of growth strata of the Changjihe Group.

Ages of fluvial terraces

The age of fluvial terraces in the valleys of the Tianshan range was extensively studied (Table 1) using optically stimulated luminescence (OSL) or electron spin resonance (ESR) (Yang et al., 2013; Lu et al., 2014; Fu et al., 2017). The age of the terraces testifies to a connection between their genesis and the uplift of the structural belts, as older terraces are found in Belt I and their age gets younger through Belts II and III. This is likely due to incision and deposition linked to the uplift phases. Although the fluvial terraces in our study area were not directly dated, the ages for the terraces in the nearby Urumqi River (Fig. 5) valley are available. There, three terrace levels were identified and assigned an age through dating of the terrace sediments by OSL and AMS^{14}C from about ~5.7 (lower and youngest terrace level), ~140 (intermediate terrace level), and ~550 ka (upper and oldest terrace level) (Zhou et al., 2002; Lu et al., 2014).

In analogy to what is observed in the Urumqi River valley, our field investigations allowed the identification of three levels of terraces associated with alluvial fans in the Toutunhe River valley (Fig. 3). From the lowest (younger) to the highest (older), we named them T1 (terrace level 1), T2 (terrace level 2), and T3 (terrace level 3). Given the vicinity of the two valleys and since both of them are located in structural Belt III, the oldest in the Tianshan range, it is reasonable to assume that the three generations of terraces in the two valleys belong to the same phases of incision/deposition and therefore can be assigned roughly similar age. Therefore, T3, T2, and T1 are assigned approximate ages of 550, 140, and 5.7 ka, respectively.

The formation of fluvial terraces is generally due to the vertical incision of a river caused by tectonic uplift (Yang and Li, 2005). Climatic fluctuations during glacial–interglacial transitions can induce the formation of fluvial terraces. The deposition and aggradation of fluvial deposits may occur in the late phases of glacial cycles, while the incision that shapes the terraces may happen near to glacial–interglacial transitions (Bridgland, 2000; Lu et al., 2010a, 2014). The advances and retreats of glaciers in the study area are evidenced by five sets of Quaternary moraines. These moraines were attributed to the Little Ice Age (~1500–1900) and the Neoglacial (~4–7 ka), Shangwangfeng (~20–40 ka), Xiawangfeng (~60–75 ka for the upper part and ~130–190 ka for the lower part), and Gaowangfeng (~470 ka) Stages, respectively (Zhao et al., 2006; Xu et al., 2010). The age of fluvial terraces allows their rough assignment to these glacial stages: T3 is approximately coincident with the Gaowangfeng Stage; T2, with the Xiawangfeng Stage; and T1, with the Neoglacial Stage (Lu et al., 2014) (Fig. 8).

Apatite fission tracks on the CM rocks, estimates of the ages of tectonic uplift and fluvial terraces, and the stratigraphic relationship between the CM rocks and the overlying sediments can provide time constraints on the activity of coal fires in the study area. According to the spatial distribution characteristics of the CM rocks and the relationship with the fluvial terraces, we divided the three combustion metamorphic zones in the study area into seven areas of distribution of CM rocks, named CM-1 to CM-7 (Fig. 3).

Table 1. **A comprehensive overview of the formation ages of fluvial terraces in the northern Tian Shan piedmont**

River	Section	Tectonic zone	Anticline	Age of fluvial terrace, ka			References
				I	II	III	
Kuitun	①	III	Dushanzi	14.98	29.3–39.2	58–75	(Yang et al., 2013)
Anjihai	②	III	Anjihai	3.6 ± 0.1	9.0 ± 0.6	53.3 ± 2.2	(Fu et al., 2017)
Manas	③	II	Manas	11.97	30.74	>31	(Yang et al., 2013)
Taxi	④	II	Tugulu	10	300	530	(Lu et al., 2010a)
Urumqi	⑤	I	Saerqiaoke	3.9 ± 0.45	142 ± 14 (T5)	550	(Lu et al., 2014)
Toutunhe	⑥	I	Kelazha	5.7	~140 (Refer to the Urumqi River)	~550 (Refer to the Urumqi River)	This study

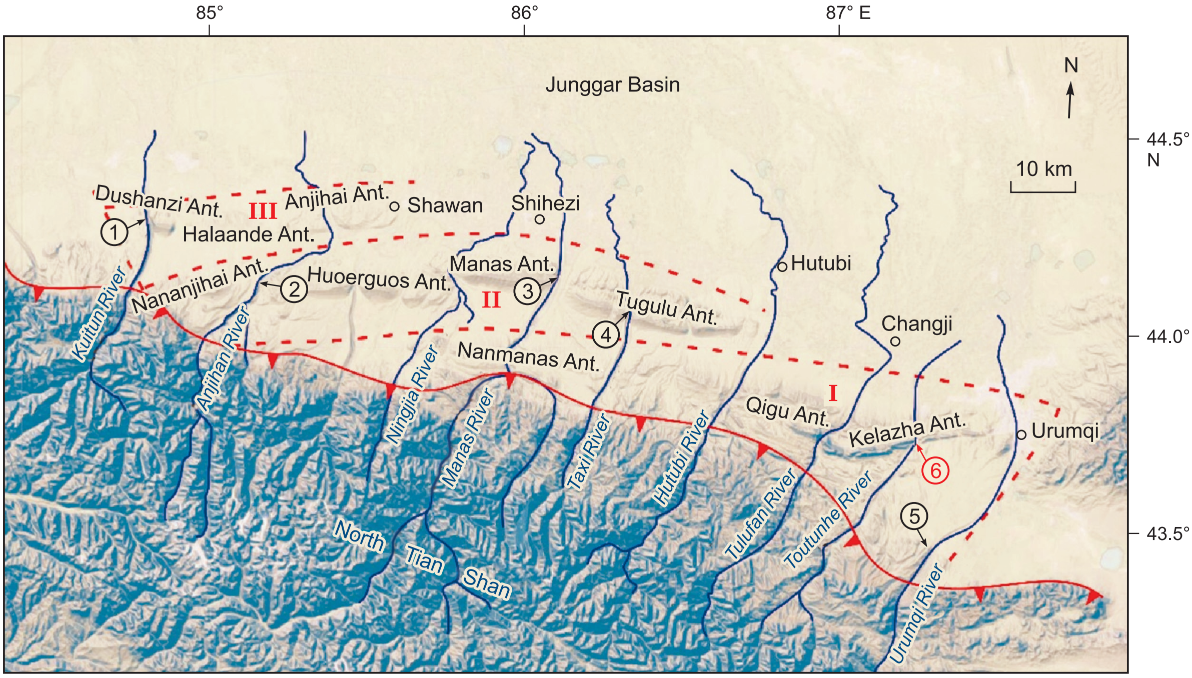

Fig. 5. Topographic map of the northern Tian Shan foreland, where three structural Belts (I, II, and III) characterize the regional topography. Numbers 1–6 indicate the sections.

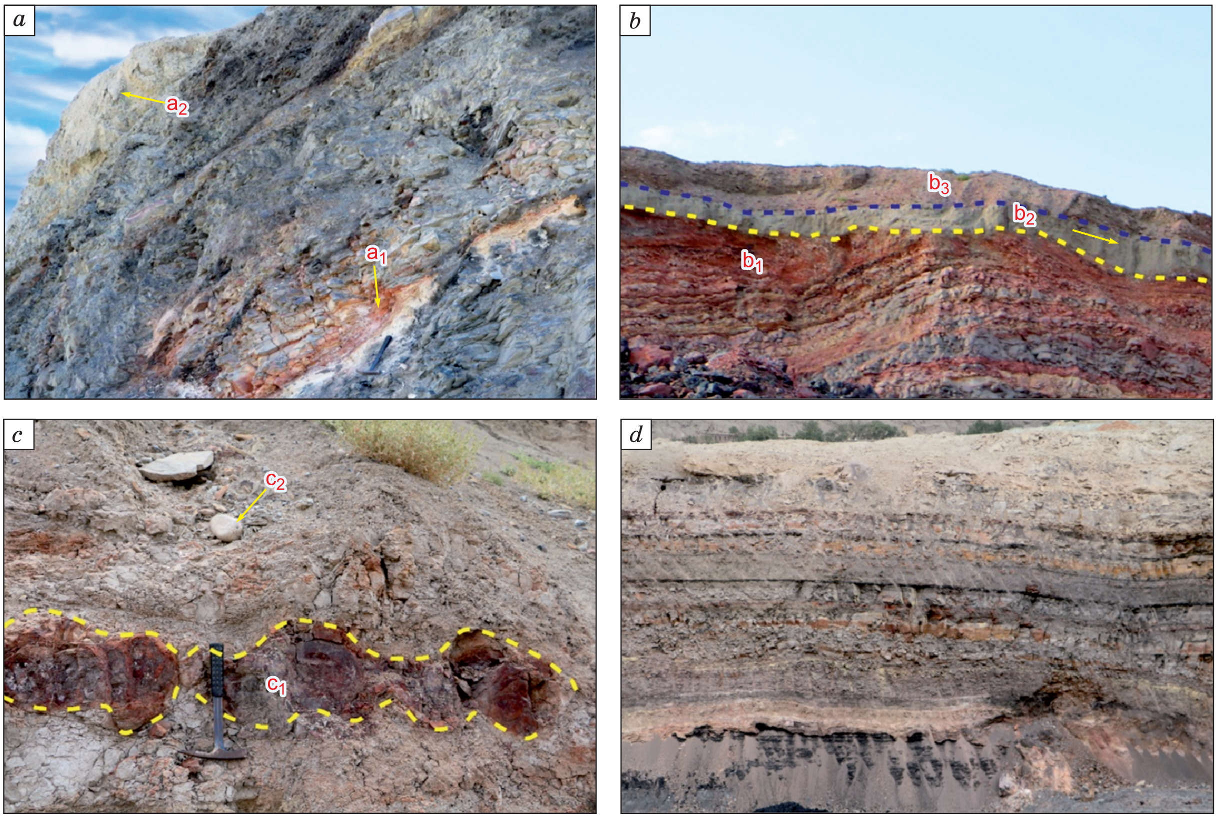

Fig. 6. Appearance of combustion metamorphic rocks.

a, Located in CM-1: a_1, red clinker; a_2, overlying sediment; *b*, photo located in CM-3; the red and black clinker have been deformed and converted owing to combustion of the coal below, and overlying terrace deposits: b_1, combustion metamorphic rocks; b_2, terrace deposits that are not baked by coal fires; b_3, gravel layer containing the CM rocks as the uppermost layer; *c*, located in CM-5: c_1, ferruginous nodules and layers; c_2, the terrace deposits that are affected by high temperatures; *d*, modern coal seam combustion due to mining.

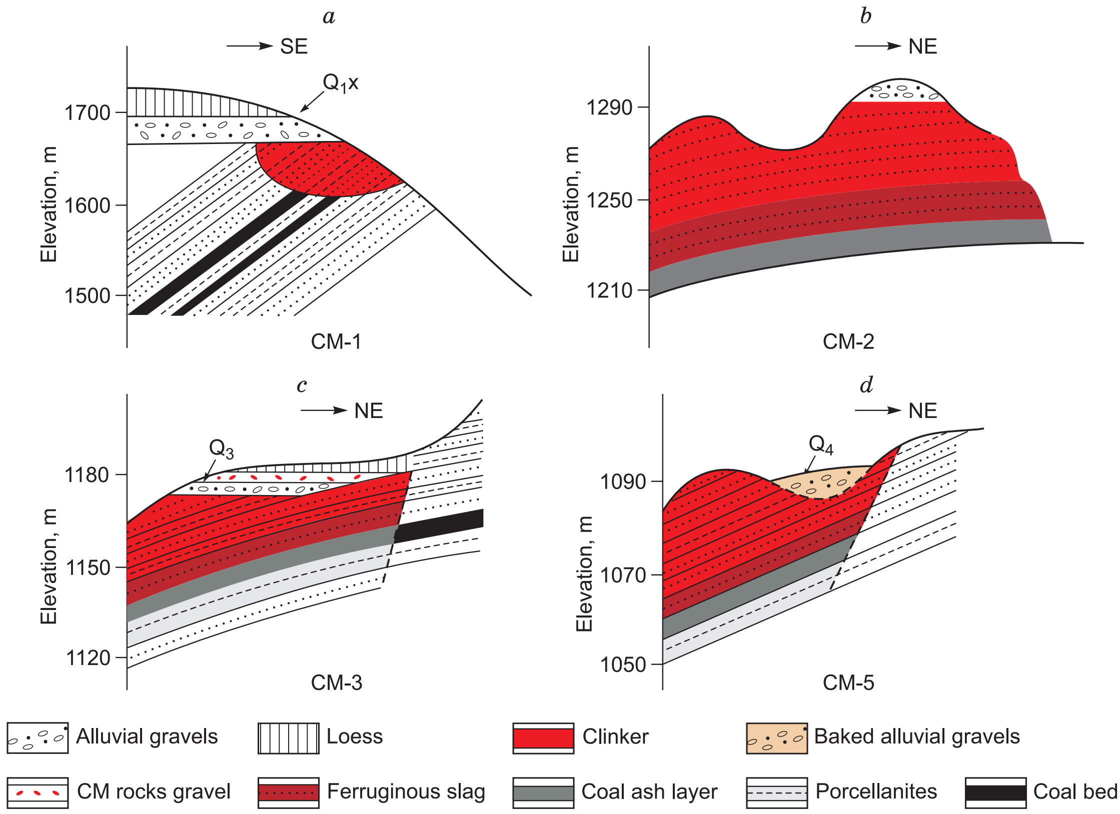

Fig. 7. The profile showing the contact relationship between CM rocks and the overlying fluvial terrace sediments.

CM-1 is located in the Kelazha area, north limb of the Kelazha Anticline (Fig. 3), 7.5 km from the Toutunhe River and 600 m above the Toutunhe River. The CM rocks are mainly distributed near the steeply dipping exposed coal seam (Fig. 6*a*), extending along the anticline strike and covered by the conglomerate of the Xiyu Formation (Q_1x). These latter do not show evidence of metamorphism (Fig. 7*a*) (Chen et al., 1994; De Boer, 1999; Sun et al., 2004; Zhang et al., 2004). Given the age of the Xiyu conglomerates (~2–3 Ma in the Taxi River section) (Sun and Zhang, 2009; Li et al., 2011a) and the fact that the conglomerates are not metamorphosed, the coal fires that produced CM-1 were active before ~2–3 Ma.

The apatite fission-track ages retrieved from the samples from CM-1 range from 5 to 24.5 Ma with a central age at 9.8 ± 1.4 and 10 ± 1.3 Ma (Fig. 4). They are much younger than the depositional age (Middle Jurassic), indicating that our samples are reset or significantly annealed. Hence, the central ages at ~9.8–10 Ma can be considered an estimate of the time the coal fire was burning. Moreover, these ages are consistent with the ages of formation of the Kelazha Anticline (Fang et al., 2007; Li et al., 2011a) (Fig. 8). We therefore presume that the coal fires of CM-1 were active during the late Miocene–Pliocene when the uplift produced structural Belt I and brought the coal seams in the Xishanyao Formation to the surface, but they terminated before 2–3 Ma (before the deposition of the Xiyu Formation conglomerates).

CM-2 is located in the Qianshuihe area with an altitude of 1250 m, 120 m above the Toutunhe River. CM-2 is located in correspondence with the highest, and therefore oldest, fluvial terrace (T3) (Fig. 3). The fluvial terrace sediments overlying the CM rocks are not metamorphosed (Fig. 7*b*). This means that the deposition/incision phase that formed the terrace occurred when those CM rocks had already formed, and therefore the coal fire responsible for their formation is older than the deposits that make up the terrace. The age of the T3 terrace is estimated to be 550 ka (Table 1); therefore the CM-5 coal fire is older than 550 ka.

The CM-3 rocks are exposed in the second terraces (T2) of the Toutunhe River (Fig. 3), 100 m above the Toutunhe River. The CM rocks are mainly red clinker and black paralavas with a thickness of 20–25 m (Fig. 6*b*). Also in this case, the overlying fluvial terrace sediments show no signs of heating, but contain clasts of CM rocks (Figs. 6*b*, 7*c*). As the river sediments covering CM-3 are not metamorphosed and the age of the second terrace (T2) was estimated at about 140 ka (Table 1), the coal fire connected with CM-3 is older than 140 ka and stopped burning before the deposition of the T2 fluvial deposits.

CM-4, in the Wanjiayao area, is located on the west side of the upper reaches of the Toutunhe River (Fig. 3), 100 m above the valley bottom. The situation is similar to that with the combustion rocks of CM-3, as the products of coal fire burning are exposed in the second fluvial terrace level (T2) and the sediments making up the terrace are not metamorphosed. Therefore, in this case the combustion phases of CM-4 can be considered older than 140 ka.

CM-5 is located on the east bank of the Toutunhe River and crops out in the scarp of the first terrace level (T1), 40 m above the Toutunhe River (Fig. 3). The CM rocks are mainly red clinker layers with ferruginous nodules (Fig. 2*b*). The thickness of the clinker varies from 50 to 100 m. The overlying Holocene alluvial deposits (Q_4) (Poisson and Avouac, 2004) show signs of metamorphism (Figs. 6*c*, 7*d*). This indicates that coal fires of CM-5 began burning after the deposition of the Holocene sediments (after the formation of the fluvial terraces of T1). Since the age of the first terrace (T1) of the Toutunhe River is 5.7 ka (Table 1), the CM-5 coal fires activity phase is younger than 5.7 ka.

CM-6 is distributed on both sides of the Qianshuihe River, which is the tributary of the Toutunhe River (Fig. 3). It is mainly composed of black paralavas and some gas-vent minerals (e.g., sulfur and sal ammoniac).

CM-7 is located in the west of the Toutunhe River, 180 m above the Toutunhe River, and distributed on both sides of the North Branch River (Fig. 3). A large amount of white smoke is visible in CM-6 and CM-7, and minerals, such as sulfur, gypsum, and calcite, nucleated along cracks and vents, indicating that the coal fires are recent.

In summary, the study area has experienced five phases of coal seam combustion (Fig. 8): the first phase occurred in the CM-1 area during the late Miocene and ended before the Pleistocene (before the deposition of the Xiyu Formation). With the erosion of the Toutunhe River, three other phases of paleo-coal fires (CM-2, -3, -4, and -5) activity occurred in the Quaternary in turn. The final burning phase is in CM-7 and -6 owing to the present mining engineering.

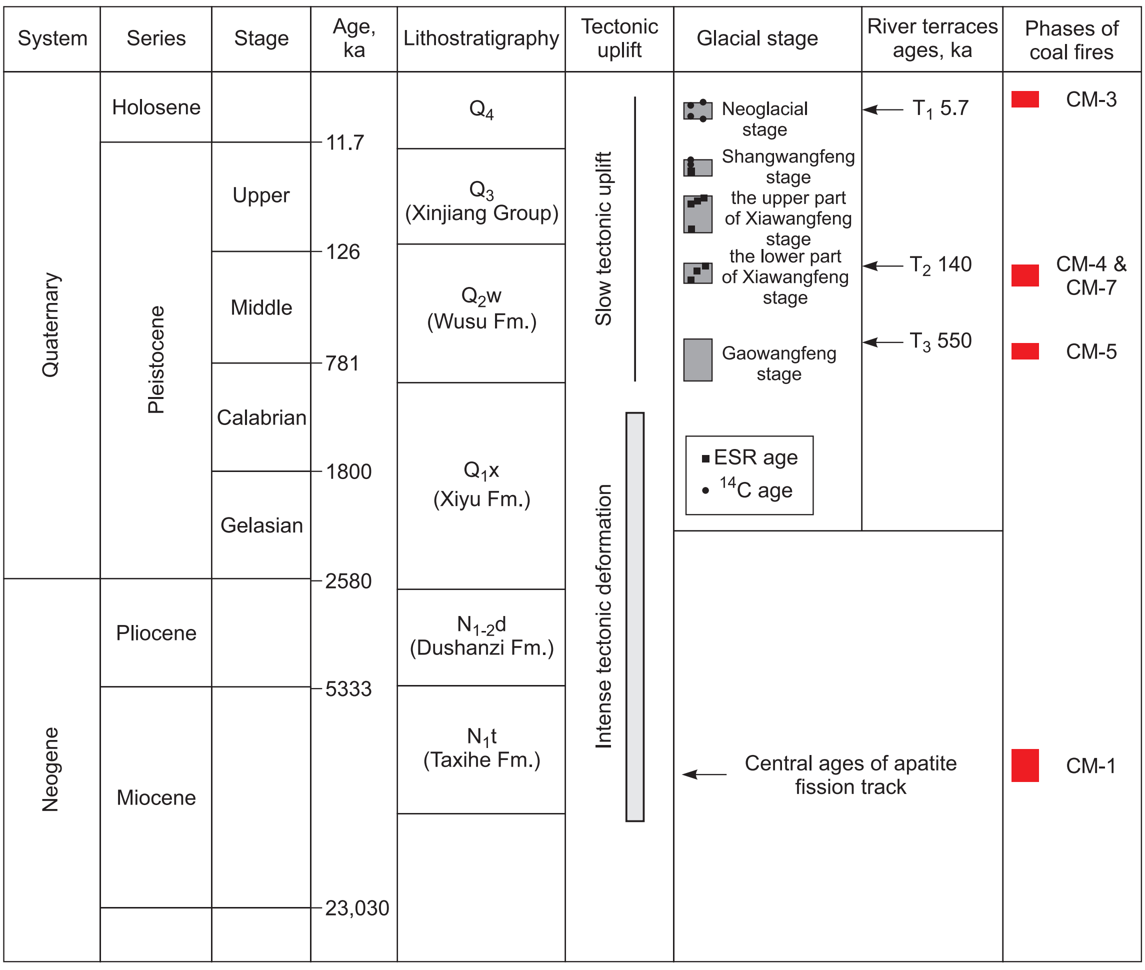

Fig. 8. The phases of combustion events. Stratigraphic chart (Fu et al., 2003). Glacial stage (Yi et al., 2004; Zhao et al., 2006; Xu et al., 2010). Fluvial terraces age (Lu et al., 2014).

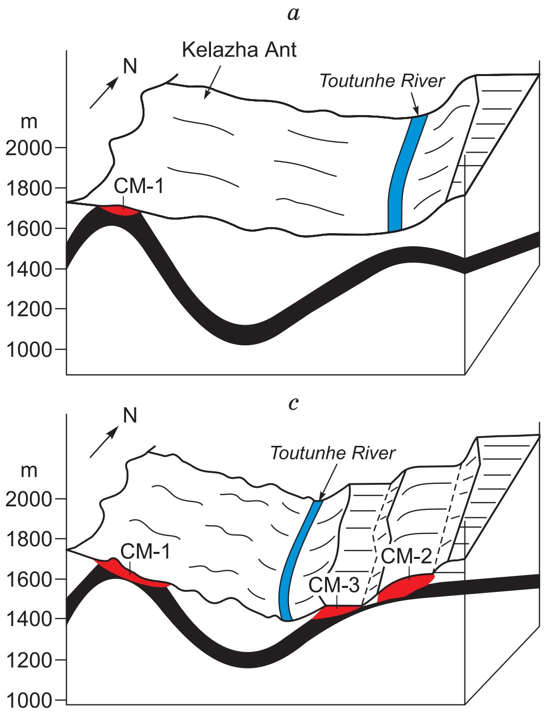

Fig. 9. Model of evolution of spontaneous combustion in a coal seam.

Evolution of paleo-coal fires

The model of evolution of coal fires in the Liuhuanggou area is shown in Fig. 9. In the late Miocene, the Kelazha Anticline formed and was eroded (Fang et al., 2007; Li et al., 2011b), causing exposure of coal seams to oxygen and creating the necessary conditions for combustion. At CM-1, through the apatite fission-track data and contact relationship of the overlying sediments, we suggest that coal seam combustion was active at about 9.8–10 Ma and stopped before the Pleistocene (Fig. 9*a*).

Since the Middle Pleistocene, progressive incision of the Toutunhe River exhumed coal seams that are now outcropping at different heights on the valley flanks. The first that were exhumed were, likely, those that now occupy the highest elevation—the pyrometamorphic rocks of CM-2. The fact that the CM-2 rocks were covered by the T3 terrace alluvial deposits and that these deposits do no show evidence of heating suggests that the coal fires had already stopped when the deposits formed (Fig. 9*b*).

Progressive incision of the valley further exposed rocks containing coal seams. Coal fires began again, and the pyrometamorphic rocks of CM-3 formed (Fig. 9*c*). A new episode of alluvial deposition at approximately 140 ka led to the accumulation of the conglomerates forming the T2 terrace. Also, no sign of metamorphism is found in the sediments above the CM-3 rocks, indicating that the coal fire had been already extinct when they deposited and were incised forming T2.

A further episode of incision led to exposure of coal seams at lower elevation. Ignition occurred again; coal fires developed, and the pyrometamorphic rocks of CM-5 formed (Fig. 9*d*). However, the alluvial deposits overlying them and forming the T1 terrace do display evidence of metamorphism. Hence, we have the evidence that the coal fire was still active when the fluvial gravels of T1 deposited, or it started burning after their deposition. This allows dating the activity phase of this coal fire between 5.7 ka and the present time.

CONCLUSIONS

The investigation and analysis of combustion metamorphic rocks in the Liuhuanggou area show the closer correlation between the coal fires and exposing conditions caused by tectonic uplift and river downcutting in the Liuhuanggou area. Based on the apatite fission-track dating combustion metamorphic rocks, the ages of tectonic uplift and fluvial terraces and contact relationship with the sediments overlying the outcrops of pyrometamorphic rocks allow reconstructing four phases of coal fire activity from Late Miocene to present. An evolution model that explains how the interplay between uplift and river incision/deposition led to the progressive exposure of coal-bearing units creating the conditions for the spontaneous ignition of coal fires.

The authors wish to thank Chaoqun Yang (China University of Geosciences, Wuhan) for providing apatite fission-track analyses and Xiaoduan Wang (Chengdu University of Technology) for helping during fieldwork. Special thanks go to the 216 Team of the Xinjiang Nuclear Bureau for aiding in the sampling and field investigations. This study is supported by the National 973 Project (No. 2015CB453001) and NSF grants (Nos. 41272131 and 41572085) of the Chinese Ministry of Science and Technology.

REFERENCES

Avouac, J.P., Tapponnier, P., Bai, M., You, H., Wang, G., 1993. Active thrusting and folding along the northern Tien Shan and late Cenozoic rotation of the Tarim relative to Dzungaria and Kazakhstan. J. Geophys. Res. B: Solid Earth 98, 6755–6804.

Bridgland, D.R., 2000. River terrace systems in north-west Europe: an archive of environmental change, uplift and early human occupation. Quat. Sci. Rev. 19, 1293–1303.

Charreau, J., Chen, Y., Gilder, S., Dominguez, S., Avouac, J., Sen, S., Sun, D., Li, Y., Wang, W., 2005. Magnetostratigraphy and rock magnetism of the Neogene Kuitun He section (northwest China): implications for Late Cenozoic uplift of the Tianshan mountains. Earth Planet. Sci. Lett. 230, 177–192.

Charreau, J., Chen, Y., Gilder, S., Barrier, L., Dominguez, S., Augier, R., Sen, S., Avouac, J.P., Gallaud, A., Graveleau, F., 2009. Neogene uplift of the Tian Shan Mountains observed in the magnetic record of the Jingou River section (northwest China). Tectonics 28, 1–22.

Chen, H., Lin, X., Guan, K., Xu, J., 1994. Early Pleistocene deposits and its lower boundary (Q/N) in Tianshan Mt., Xinjiang Region. Quat. Sci. 1, 38–47.

Chen, S., Qi, J., Yu, F.S., Yang, Q., 2007. Deformation characteristics in the southern margin of the Junggar Basin and their controlling factors. Acta Geol. Sin. 81, 151–157.

Chen, Z., Lu, K., Wang, G., Chen, B., Zheng, E., Cui, L., Ding, W., 2010. Characteristics of Cenozoic structural movements in southern margin of Junggar basin and its' relationship to the mineralization of sandstone-type uranium deposits. Acta Petrol. Sin. 26 (2), 457–470.

Daëron, M., Avouac, J., Charreau, J., 2007. Modeling the shortening history of a fault tip fold using structural and geomorphic records of deformation. J. Geophys. Res. B: Solid Earth 112, 1–19.

De Boer, C., 1999. Rock-magnetic Studies on Hematite, Maghemite and Combustion-Metamorphic rocks. Utrecht Univ., pp. 193–200.

Delvaux, D., Cloetingh, S., Beekman, F., Sokoutis, D., Burov, E., Buslov, M.M., Abdrakhmatov K.E., 2013. Basin evolution in a folding lithosphere: Altai–Sayan and Tien Shan belts in Central Asia. Tectonophysics 602, 194–222.

Dobretsov, N.L., Buslov, M.M., Delvaux, D., Berzin, N.A., Ermikov, V.D., 1996. Meso- and Cenozoic tectonics of the Central Asian mountain belt: effects of lithospheric plate interaction and mantle plume. Int. Geol. Rev. 38, 430–466.

Fang, S., Song, Y., Jia, C., Guo, Z., Zhang, Z., Liu, L., 2007. Timing of Cenozoic intense deformation and its implications for petroleum accumulation, northern margin of Tianshan Orogenic Belt, Northwest China. Earth Sci. Front. 14 (2), 205–214.

Fu, B., Lin, A., Kano, K.-i., Maruyama, T., Guo, J., 2003. Quaternary folding of the eastern Tian Shan, northwest China. Tectonophysics 369, 79–101.

Fu, X., Li, S., Li, B., Fu, B., 2017. A fluvial terrace record of late Quaternary folding rate of the Anjihai anticline in the northern piedmont of Tian Shan, China. Geomorphology 278, 91–104.

Glorie, S., De Grave, J., 2016. Exhuming the Meso-Cenozoic Kyrgyz Tianshan and Siberian Altai-Sayan: A review based on low-temperature thermochronology. Geosci. Front. 7, 155–170.

Gong, Z.J., Li, S.H., Li, B., 2014. The evolution of a terrace sequence along the Manas River in the northern foreland basin of Tian Shan, China, as inferred from optical dating. Geomorphology 213, 201–212.

Gong, Z.J., Li, S.H., Li, B., 2015. Late Quaternary faulting on the Manas and Hutubi reverse faults in the northern foreland basin of Tian Shan, China. Earth Planet. Sci. Lett. 424, 212–225.

Grave, J.D., Buslov, M.M., Haute, P.V.D., 2007. Distant effects of India–Eurasia convergence and Mesozoic intracontinental deformation in Central Asia: Constraints from apatite fission-track thermochronology. J. Asian Earth Sci. 29, 188–204.

Guan, H., Van Ganderen, J., Tan, Y., Kang, G., Wan, Y., 1998. The Environment Investigation and Study of Coal Seam Self-Combustion in Northern China. Coal Industrial Press, Beijing, pp. 27–28.

Guo, Z., Fang, S., Zhang, R., Zhang, Z., Wu, C., Shao, K., 2006. Growth strata and their application in timing deformation of foreland thrust-fold belts in the north margin of Tianshan. Oil Gas Geol. 27, 475–481.

Guo, Z., Deng, S., Wei, G., 2007. Comparative study of the foreland thrust belts of South and North Tianshan and implications for hydrocarbon accumulation. Earth Sci. Front. 14, 123–131.

Gur, D., Steinitz, G., Kolodny, Y., Starinsky, A., McWilliams, M., 1995. ^{40}Ar^{39}Ar dating of combustion metamorphism ("Mottled Zone", Israel). Chem. Geol. 122 (1–4), 171–184.

Heffern, E.L., Coates, D.A., 2004. Geologic history of natural coal-bed fires, Powder River basin, USA. Int. J. Coal Geol. 59, 25–47.

Heffern, E.L., Reiners, P.W., Naeser, C.W., Coates, D.A., 2007. Geochronology of clinker and implications for evolution of the Powder River Basin landscape, Wyoming and Montana, in: Stracher, G.B. (Ed.), Geology of Coal Fires: Case Studies from Around the World. GSA, Boulder, Colo., pp. 155–176.

Hoffmann, J., Roth, A., Voigt, S., 2003. Detecting coal fires in China using differential interferometric synthetic aperture radar (InSAR), in: Proc. Fringe Workshop (ESA SP-550), Frascati, Italy, pp. 1–5.

Huang, S., Qin, M., Liu, Z., Mao, L., He, Z., Xu, Q., 2016. Fluid inclusion and organic geochemistry characteristics of uranium-bearing sandstone in the Liuhuanggou area in the southern margin of Junggar Basin. Acta Geol. Sin. 90 (3), 475–488.

Ji, J., Luo, P., White, P., Jiang, H., Gao, L., Ding, Z., 2008. Episodic uplift of the Tianshan Mountains since the late Oligocene constrained by magnetostratigraphy of the Jingou River section, in the southern margin of the Junggar Basin, China. J. Geophys. Res. B: Solid Earth 113, 1–14.

Jiang, K.Q., Tian, J.J., Wang, L.J., Peng, X.F., Wang, W., 2010. Sedimentary characteristics and coal-accumulation pattern of the Xishanyao Formation in southern margin area of Junggar Basin. Geoscience 24, 1204–1212.

Kong, F., Li, W., Huang, X., 2006. Characters of distributions and reasons analysis of ill geological phenomena in the Toutunhe River basin. Sci. Soil Water Conserv. 4 (5), 35–39.

Kuenzer, C., Stracher, G.B., 2012. Geomorphology of coal seam fires. Geomorphology 138, 209–222.

Kuenzer, C., Zhang, J., Tetzlaff, A., van Dijk, P., Voigt, S., Mehl, H., Wagner, W., 2007. Uncontrolled coal fires and their environmental impacts: Investigating two arid mining regions in north-central China. Appl. Geogr. 27, 42–62.

Li, C., Guillaume, D.V., Guo, Z., 2011a. Magnetostratigraphy of the Northern Tian Shan foreland, Taxi He section, China. Basin Res. 23, 101–117.

Li, C., Guo, Z., Guillaume, D.V., 2011b. Late Cenozoic tectonic deformation across the northern foreland of the Chinese Tian Shan. J. Asian Earth Sci. 42, 1066–1073.

Li, Y., Cao, D., Wei, Y., Wang, A., Zhang, Q., Wu, P., 2016. Middle to low rank coalbed methane accumulation and reservoiring in the southern margin of Junggar Basin. Acta Petrol. Sin. 37 (12), 1472–1482.

Liu, Z., Qin, M., He, Z., Guo, Q., Xu, Q., Geng, Y., Deng, G., 2017. Tectonic uplift-denudation inhomogeneity and impacts on the sandstone-hosted uranium mineralization in the southern margin of the Junggar Basin. Geotectonica et Metallogenia 41, 853–864.

Lu, H., Burbank, D.W., Li, Y., 2010a. Alluvial sequence in the north piedmont of the Chinese Tian Shan over the past 550 kyr and its relationship to climate change. Palaeogeogr. Palaeoclimatol. Palaeoecol. 285 (3–4), 343–353.

Lu, H., Burbank, D.W., Li, Y., Liu, Y., 2010b. Late Cenozoic structural and stratigraphic evolution of the northern Chinese Tian Shan foreland. Basin Res. 22, 249–269.

Lu, H., Zhang, T., Zhao, J., Si, S., Wang, H., Chen, S., Zheng, X., Li, Y., 2014. Late Quaternary alluvial sequence and uplift-driven incision of the Urumqi River in the north front of the Tian Shan, northwestern China. Geomorphology 219, 141–151.

Molnar, P., Tapponnier, P., 1975. Cenozoic tectonics of Asia: effects on a continental collision. Science 189, 419–426.

Molnar, P., England, P., Martinod, J., 1993. Mantle dynamics, uplift of the Tibetan Plateau, and the Indian Monsoon. Rev. Geophys. 31, 357–396.

Novikov, I.S., 2013. Reconstructing the stages of orogeny around the Junggar basin from the lithostratigraphy of Late Paleozoic, Mesozoic, and Cenozoic sediments. Russ. Geol. Geophys. 54 (2), 138–152, doi: 10.1016/j.rgg.2013.01.002.

Novikov, I.S., Sokol, E.V., 2007. Combustion metamorphic events as age markers of orogenic movements in Central Asia. Acta Petrol. Sin. 23, 1561–1572.

Novikov, I.S., Sokol, E.V., Travin, A.V., Novikova, S.A., 2008. Signature of Cenozoic orogenic movements in combustion metamorphic rocks: mineralogy and geochronology (example of the Salair-Kuznetsk Basin transition). Russ. Geol. Geophys. 49 (6), 378–396, doi: 10.1016/j.rgg.2007.11.011.

Novikova, S., Sokol, E.V., Khvorov, P., 2016. Multiple combustion metamorphic events in the Goose Lake Coal Basin, Transbaikalia, Russia: First dating results. Quat. Geochronol. 36, 38–54.

Poisson, B., Avouac, J.P., 2004. Holocene hydrological changes inferred from alluvial stream entrenchment in North Tian Shan (Northwestern China). J. Geol. 112, 231–249.

Querol, X., Izquierdo, M., Monfort, E., Alvarez, E., Font, O., Moreno, T., Alastuey, A., Zhuang, X., Lu, W., Wang, Y., 2008. Environmental characterization of burnt coal gangue banks at Yangquan, Shanxi Province, China. Int. J. Coal Geol. 75, 93–104.

Reiners, P.W., Riihimaki, C.A., Heffern, E.L., 2011. Clinker geochronology, the first glacial maximum, and landscape evolution in the northern Rockies. GSA Today 21 (7), 4–9.

Ribeiro, J., Suárez-Ruiz, I., Ward, C.R., Flores, D., 2016. Petrography and mineralogy of self-burning coal wastes from anthracite mining in the El Bierzo Coalfield (NW Spain). Int. J. Coal Geol. 154–155, 92–106.

Riihimaki, C.A., Reiners, P.W., Heffern, E.L., 2009. Climate control on Quaternary coal fires and landscape evolution, Powder River basin, Wyoming and Montana. Geology 37, 255–258.

Scharer, K.M., Burbank, D.W., Chen, J., Weldon, R.J., Rubin, C., Zhao, R., Shen, J., 2004. Detachment folding in the Southwestern Tian Shan–Tarim foreland, China: shortening estimates and rates. J. Struct. Geol. 26, 2119–2137.

Silva, L.F.O., Boit, K.M.D., 2011. Nanominerals and nanoparticles in feed coal and bottom ash: implications for human health effects. Environ. Monit. Assess. 174, 187–197.

Sokol, E.V., Volkova, N.I., 2007. Combustion metamorphic events resulting from natural coal fires, in: Stracher, G.B. (Ed.), Geology of Coal Fires: Case Studies from Around the World. GSA, Boulder, Colo., pp. 97–115.

Sokol, E.V., Novikova, S.A., Alekseev, D.V., Travin, A.V., 2014. Natural coal fires in the Kuznetsk Coal Basin: Geologic causes, climate, and age. Russ. Geol. Geophys. 55 (9), 1043–1064, doi: 10.1016/j.rgg.2014.08.001.

Song, Z., Kuenzer, C., 2014. Coal fires in China over the last decade: A comprehensive review. Int. J. Coal Geol. 133, 72–99.

Song, Z., Kuenzer, C., 2017. Spectral reflectance (400–2500 nm) properties of coals, adjacent sediments, metamorphic and pyrometamorphic rocks in coal-fire areas: A case study of Wuda coalfield and its surrounding areas, northern China. Int. J. Coal Geol. 171, 142–152.

Stracher, G.B., 2007. The origin of gas-vent minerals: Isochemical and mass-transfer processes, in: Stracher, G.B. (Ed.), Geology of Coal Fires: Case Studies from Around the World. GSA, Boulder, Colo., pp. 91–96.

Stracher, G.B., Taylor, T.P., 2004. Coal fires burning out of control around the world: thermodynamic recipe for environmental catastrophe. Int. J. Coal Geol. 59, 7–17.

Stracher, G.B., Prakash, A., Sokol, E.V., 2015. Coal and Peat Fires: a Global Perspective, Vol. 3: Case Studies–Coal Fires. Elsevier, Amsterdam.

Sun, J., Zhang, Z., 2009. Syntectonic growth strata and implications for late Cenozoic tectonic uplift in the northern Tian Shan, China. Tectonophysics 463, 60–68.

Sun, J., Zhu, R., Bowler, J., 2004. Timing of the Tianshan Mountains uplift constrained by magnetostratigraphic analysis of molasse deposits. Earth Planet. Sci. Lett. 219, 239–253.

Sun, Q., Sun, B., Sun, F., Yang, Q., Chen, G., Yang, M., 2012. Accumulation and geological controls of low-rank coalbed methane in southeastern Junggar Basin. Geol. J. China Univ. 18, 460–464.

Tapponnier, P., Xu, Z.Q., Roger, F., Meyer, B., Arnaud, N., Wittlinger, G., Yang, J.S., 2001. Oblique stepwise rise and growth of the Tibet plateau. Science 294 (5547), 1671–1677.

Voigt, S., Tetzlaff, A., Zhang, J., Künzer, C., Zhukov, B., Strunz, G., Oertel, D., Roth, A., van Dijk, P., Mehl, H., 2004. Integrating satellite remote sensing techniques for detection and analysis of uncontrolled coal seam fires in North China. Int. J. Coal Geol. 59, 121–136.

Wang, H., Dlugogorski, B.Z., Kennedy, E.M., 2003. Coal oxidation at low temperatures: oxygen consumption, oxidation products, reaction mechanism and kinetic modelling. Prog. Energy Combust. Sci. 29 (6), 487–513.

Wu, T.W., Tian, J.J., Ri, M.Z., Chen, B., 2012. Analysis of CBM deposit law of 3# mine, Liuhuanggou coal mine in Changji, Xinjiang. Geol. Sci. Technol. Inf. 31, 7.

Xu, Q.Q., Ji, J.Q., Xu, J.Y., Hou, J.J., 2015. Cenozoic continental deformation in northern China and its geodynamic mechanism. Geol. China 6, 1633–1673.

Xu, X., Kleidon, A., Miller, L., Wang, S., Wang, L., Dong, G., 2010. Late Quaternary glaciation in the Tianshan and implications for palaeoclimatic change: a review. Boreas 39, 215–232.

Yang, J.C., Li, Y.L., 2005. Fundamentals of Geomorphology [in Chinese]. Peking Univ. Press, Beijing.

Yang, X., Li, A., Hunag, W., 2013. Uplift differential of active fold zones during the late Quaternary, northern piedmonts of the Tianshan Mountains, China. Sci. China, Ser. D. Earth Sci. 56, 794–805.

Yi, C., Liu, K., Cui, Z., Jiao, K., Yao, T., He, Y., 2004. AMS radiocarbon dating of late Quaternary glacial landforms, source of the Urumqi River, Tien Shan–a pilot study of ^{14}C dating on inorganic carbon. Quat. Int. 121, 99–107.

Zhang, X., Kroonenberg, S.B., De Boer, C.B., 2004. Dating of coal fires in Xinjiang, north-west China. Terra Nova 16, 68–74.

Zhang, Z.C., 2015. Study on flood characteristics of Toutun River Basin of Xinjiang. Water Conserv. Sci. Technol. Econ. 21, 92–94.

Zhao, J., Zhou, S., He, Y., Ye, Y., Liu, S., 2006. ESR dating of glacial tills and glaciations in the Urumqi River headwaters, Tianshan Mountains, China. Quat. Int. 144, 61–67.

Zhou, S.D., Liu, D.M., Sun, S.H., Cai, Y.D., 2015. Factors affecting coalbed methane enrichment and CBM favorable area of Liuhuanggou area in the southern Jungger Basin. Geoscience 29 (1), 179–189.

Zhou, S.Z., Jiao, K.Q., Zhao, J.D., Zhang, S.Q., Cui, J.X., Xu, L.B., 2002. Geomorphology of the Urümqi River Valley and the uplift of the Tianshan Mountains in Quaternary. Sci. China, Ser. D. Earth Sci. 45, 961–968.

Поступила в редакцию 9 марта 2020 г.,
принята в печать 29 июня 2020 г.